Marie Skłodowska-Curie (MSCA) – Innovative Training Networks (ITN)
H2020-MSCA-ITN European Training Networks

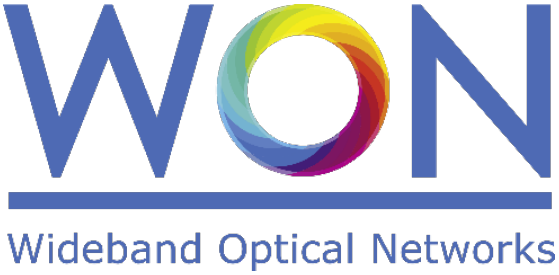

Wideband Optical Networks [WON]

Grant agreement ID: 814276

WP3: In-line components design
Deliverable D3.1: Design of wideband add/drop switching node architecture

This project has received funding from the European Union's Horizon 2020 research and innovation programme under the Marie Skłodowska-Curie grant agreement 814276.

Document Details

Work Package	WP3: In-line components design
Deliverable number	D3.1
Deliverable Title	Design of wideband add/drop switching node architecture
Lead Beneficiary:	Technische Universiteit Eidhoven, TUE
Deliverable due date:	30/06/2020
Actual delivery date:	14/12/2020
Dissemination level:	Public

Project Details

Project Acronym	WON
Project Title	Wideband Optical Networks
Call Identifier	H2020-MSCA-2018 Innovative Training Networks
Coordinated by	Aston University, UK
Start of the Project	1 January 2019
Project Duration	48 months
WON website:	https://won.astonphotonics.uk/
CORDIS Link	https://cordis.europa.eu/project/rcn/218205/en

WON Consortium and Acronyms

Consortium member	**Legal Entity Short Name**
Infinera Germany	INF G
Aston University	Aston
Danmarks Tekniske Universitet	DTU
VPIphotonics GmbH	VPI
Infinera Portugal	INF PT
Fraunhofer HHI	HHI
Politecnico di Torino	POLITO
Technische Universiteit Eidhoven	TUE
Universiteit Gent	UG
Keysight Technologies	Keysight
Finisar Germany GmnH	Finisar
Orange SA	Orange
Technische Universitaet Berlin	TUB
Instituto Superior Tecnico, University of Lisboa	IST

Abbreviations

EC:	European Commission
ETN:	European Training Network
GA:	Grant Agreement
WSS:	Wavelength Selective Switch
DWDM:	Dense Wavelength Division Multiplexing
IEGS:	Integrated Echelle Gratings
RC:	Rowland Circle
IMOS:	Indium Phosphide membrane on Silicon
SOI:	Silicon on Insulator
AWGs:	Arrayed waveguide gratings
FSR:	Free Spectral Range
PDLS:	Polarization Dependent Losses
TOC:	Thermo-Optic Coefficient
TOE:	Thermo-Optic Effect
MZIS:	Mach-Zehnder Interferometers

Contents

LIST OF FIGURES

EXECUTIVE SUMMARY

The present scientific deliverable is part of the Work Package 3 “In-line components design” of the ETN project WON “Wideband Optical Network”, funded under the Horizon 2020 Marie Sklodowska-Curie scheme Grant Agreement 814276.

The document provides details derived on the concept of an add/drop switching node. An add/drop switching node suitable for wideband metro/access and based on novel low-port count integrated wavelength selective switch is presented. The concept for the node has two main building blocks, integrated echelle gratings / array waveguide gratings for wavelength multiplexing/ demultiplexing and thermo-optic switches as the switching elements. Simulation and experimental results regarding both blocks show wideband operation, from the O-, to the L-Band, while maintaining several critical parameters such as, insertion loss, crosstalk, number of channels and footprint like C-band only, currently deployed, add/drop switching nodes.

1. Overview of the add/drop switching node architecture

Optical add/drop switching nodes exploiting *wavelength selective switch* (WSS) modules are largely employed in telecom networks for flexible spectrum allocation and routing. Most of the commercial WSS modules can only work in the C or L-band. In order to fulfil the requirements of the next generation networks, multiband, high bandwidth, low power consumption, low costs as well as data rate and format independent all-optical switching technology is required.

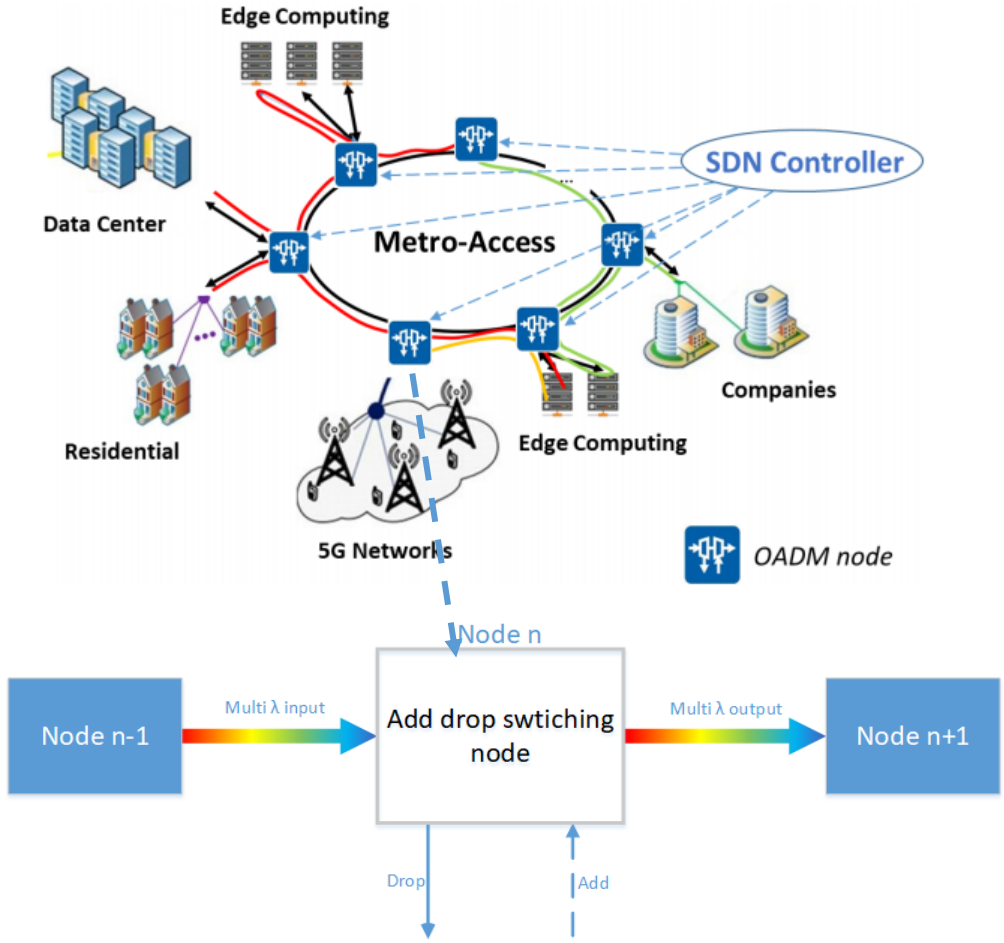

Figure 1. Concept of an Add/Drop Switching Node [1]

In a add drop switching node, optical signals are selectively dropped or inserted in a transparent WDM network. As its name suggests, the add drop node can add one or more wavelength channels to an existing multi-channel WDM signal, or at the same time, drop one or more channels, moving it to another network path. A high-level view of the add drop switching node is shown on Figure 1 and Figure 2.

There is a need for low-cost 2-degree add/drop switching nodes in Metro-Access networks [2]. Figures 1 and in Figure 2 illustrate the typical structure of the node. In the add/drop switching node, an optical input, comprised of multiple wavelength channels is first pre-amplified to compensate the propagation losses from node n-1 to node n, after that the WDM light is separated into its individual components, followed by a section where the wavelengths to be dropped/bypassed are selected. After that there is a path for the adding of channels followed by the recombination of the channels into

WDM light. Finally, a post-amplifier is used to compensate the losses of the optical add/drop switching node.

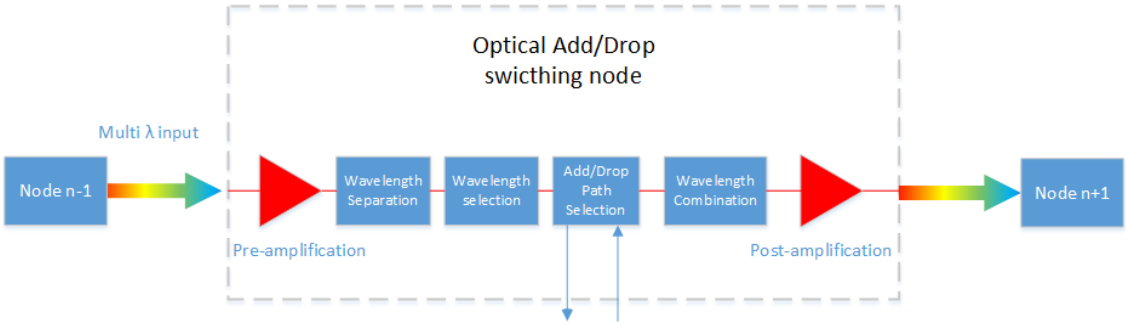

Figure 2.Typical add drop switching node architecture

The add-drop switching node depicted on Figure 2 would usually be implemented as five individual components (one per band) for each of the blocks (wavelength separation, selection, insertion and (re)combination). Novel integrated WSSs presents themselves as attractive alternatives for ideally implementing the functions of wavelength separation, selection, adding/dropping, wavelength re-combination and also on-chip amplification [3] to compensate for the node losses. Photonic integration paves the way for making low-cost, low-port count WSSs with several functions implemented on a single chip, that are specifically important for the metro/access networks due to the large amount of WSSs to be deployed. Wideband WSSs are therefore an important alternative in order to reducing the component count, the footprint, and power consumption of the switching node.

2. Design of the wavelength demultiplexing and multiplexing

One of the ways of separating WDM channels into their individual components is by means of a diffraction grating. In a diffraction grating, the incident polychromatic light is dispersed, and each wavelength is diffracted to a different angle. One of the promising technologies for wavelength demultiplexing on integrated photonics are *integrated echelle gratings* (IEGs) [3]. Ultra-low-loss, low-crosstalk, high channel count and polarization insensitive IEGs have been successfully demonstrated [4]. Being bi-directional devices, IEGs can also be operated in reverse mode, i.e individual channels at the inputs are combined into a WDM signal at the output.

On an IEG, equally spaced grooves are formed on a reflective coating and deposited on a substrate. The dispersion performance and efficiency of the IEG depends on the facet period and its angle. The concave grating facets are mounted on a circular section whose radius is twice that of a circle, called the *Rowland Circle* (RC), where the input and output waveguides are mounted. As seen from Figure 3, the diverging incident light beam is focused from the input waveguides on the RC and each spectral component of the diffracted light is focused to a different position and output waveguide.

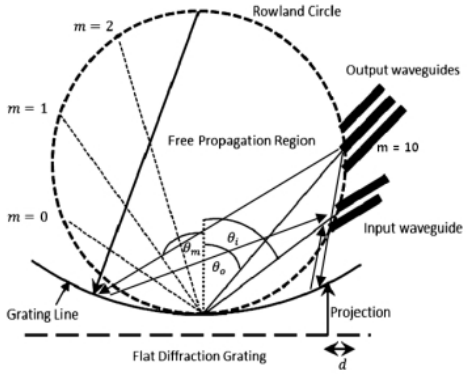

Figure 3. Rowland Circle.

The Indium Phosphide membrane on silicon (IMOS) platform developed at Eindhoven University of Technology showed potential to achieve enhanced optical confinement in both active and passive devices. It is based on a vertical integration scheme, where active and passive layers couple strongly, allowing active devices to be independently optimized while maintaining the performance and footprint of passive waveguides - very close to what is seen on pure SOI platforms.

For multiplexer/demultiplexer part of the add/drop switching node, a total of 5 IEGs, from the O- to the L-band, with 30 channels and 100 GHz channel spacing, were designed with aluminium used as a material for the reflective layer, given its broadband reflectivity. The simulation results for TE polarized light show losses better than -3 dB at all bands, with the lowest loss at the C-band (-1.5 dB), and highest at the O-band (-2.5 dB). The simulated devices also had a small footprint with a grating length of 11000 μm and grating radius of 3000 μm. The simulation results are summarized on Table 1 and on Figures 4-8.

Optical Band	Peak loss (dB)	Number of Channels	Channel Spacing (GHz)	Grating Radius / Length (μm)
O	-2.5	30	100	3000/11000
E	-2	30	100	3000/11000
S	-1.6	30	100	3000/11000
C	-1.5	30	100	3000/11000
L	-1.7	30	100	3000/11000

Table 1.IEGs performance across multiple bands.

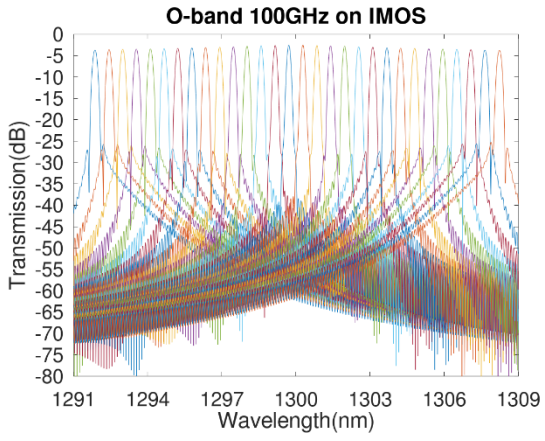

Figure 4. O-Band

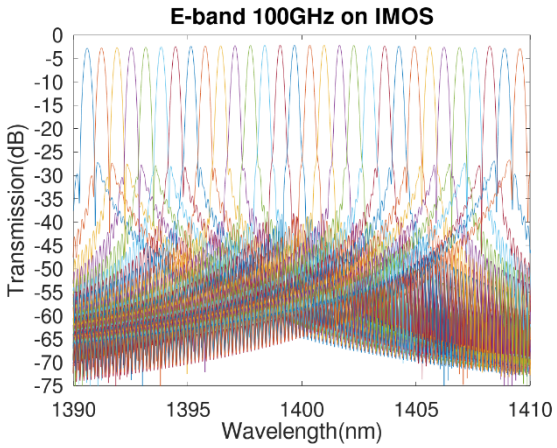

Figure 5. E-Band

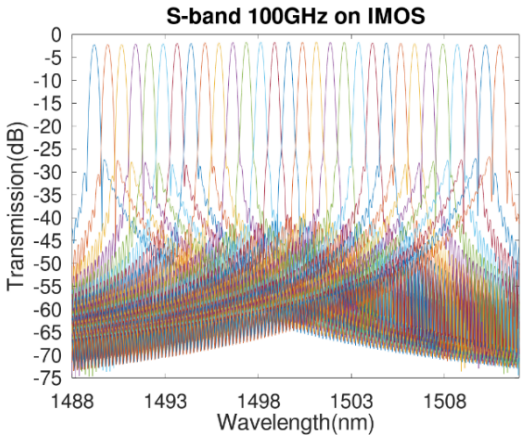

Figure 6. S-Band

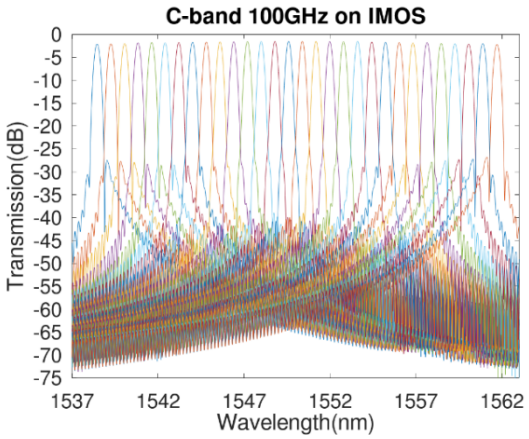

Figure 7. C-Band

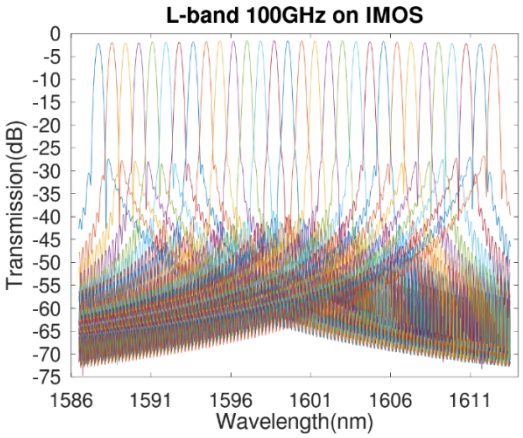

Figure 8. L-band Transmission

A second optical component that can be used for optical (de-)multiplexing of the WDM channels is the *arrayed waveguide-grating* (AWG) [5]. Low loss and low crosstalk, polarization insensitive integrated AWGs on a SOI platform also presents an attractive solution for future wideband add-drop switching nodes. We have *reported polarization dependent losses* (PDLs) as low as 0.28 dB insertion losses smaller than – 3.5 dB and crosstalk levels below -35 dB [6]. All of this, while maintaining a small footprint due to the 3-μm SOI platform as shown in Figure 9a. On Figures 9b and 9c we show the transmission spectra for the TE and TM modes for S-, C- and L-bands that highlight the good performance of these devices,

The multiband operation of the AWGs and IEGs can then be employed in the node architectures shown in Figure 2.

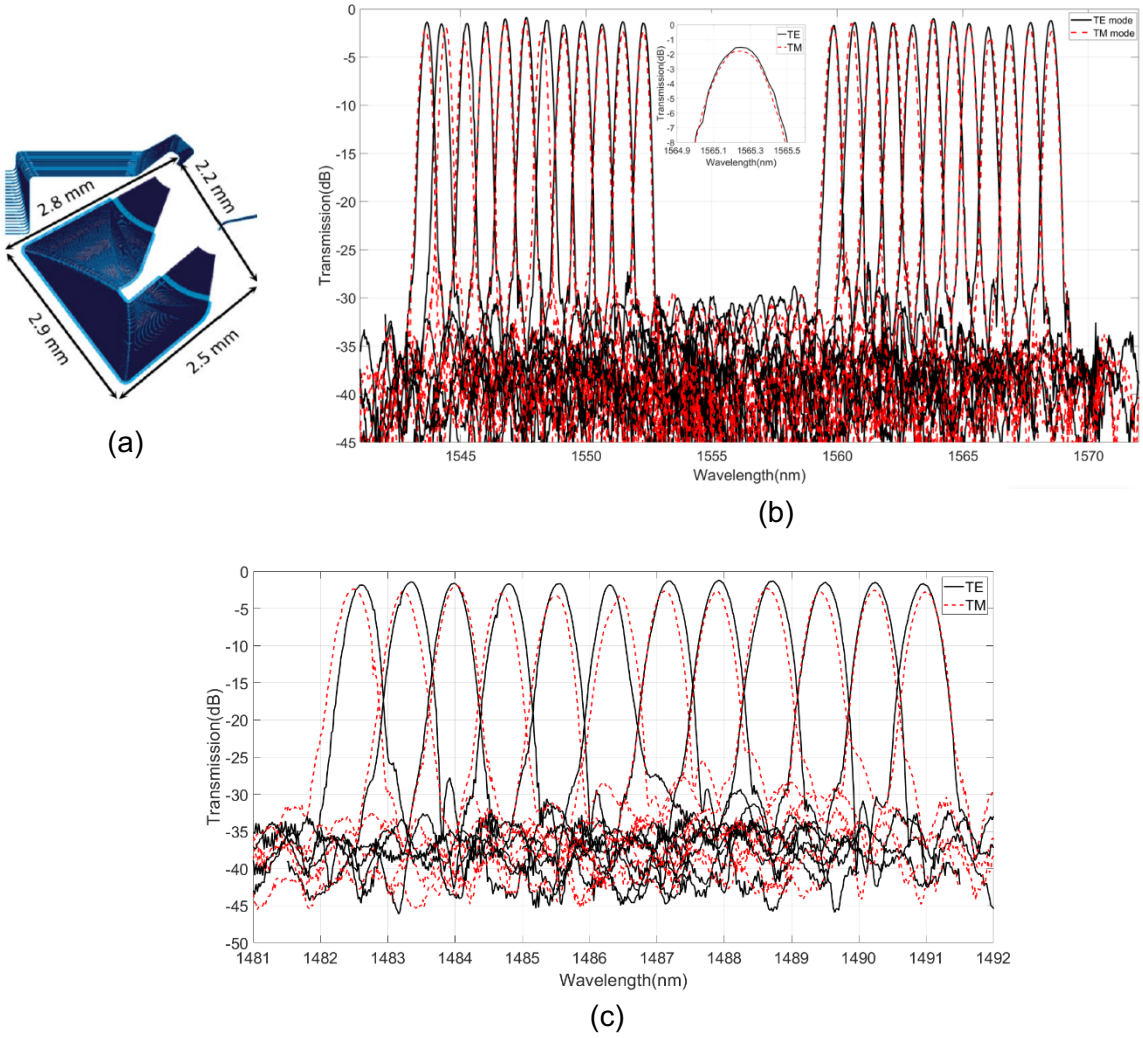

Figure 9. (a) Layout of the Fabricated AWG; (b) Power transmission Spectra for TE and TM Modes at the C and L-band; (c) Power transmission spectra for TE and TM modes at the S-band [6].

3. Wideband wavelength switching

The second stage of the switching node is usually comprised of a section for wavelength selection, i.e a switching section. An optical switch works by selectively switching an optical signal from one node, or circuit, to another, in response to supervisory control signals. There are several methods for realizing an optical switch and each rely on different physical mechanism for its operation. Several types of optical switches have been proposed as, electro-optical switches, thermo-optical switches, switches based on micro-mirrors [7], on semiconductor optical amplifiers [1], among others [8]. Among those, thermo-optical switches present themselves as an attractive approach for a wideband switching element mainly due to the low variability of the *Thermo-Optic Coefficient* (TOC) with wavelength [9].

Silica based devices, derived from the well-established silica-on-silicon technology have been demonstrated [10] and are especially interesting because of the good heat conduction characteristics of silicon that allow the substrate itself to act as a good heat sink.

The switching between output channels in a Thermo-Optical Switch is induced by creating a difference in their effective refractive index and it is achieved by applying heat on the desired

waveguide by means of electrodes deposited on top of the waveguides. This change in the refractive index is due to the *thermo-optic effect* (TOE), an effect that occurs in all materials, and the TOC, given by, dn/dt, that is the rate of change in the refractive index in response to a change in temperature.

A theoretical model for describing the temperature dependence of the refractive index is seen on [6][7], and it is a form of the Sellmeier relation that represents the product of the refractive index and the thermo-optic coefficient, and is given by:

$$2n\frac{dn}{dT} = GR + HR^2$$

Where, $R = \lambda^2/(\lambda^2 - \lambda_{ig}^2)$, is the normalized dispersive wavelength.

This model is physically meaningful because it comes from a set of measured optical parameters, where G is related to the thermal expansion coefficient and H is related to the temperature coefficient of the excitonic band gap. The value for these constants can be found on [11] for several crystals and glasses. Using these values, we evaluated $2n(dn/dt)$ for Silica and Silicon for wavelengths on the O-band to the L-band and the results are shown on Figures 10a for crystalline Silicon (c-Si) and 10b for Silica (SiO_2).

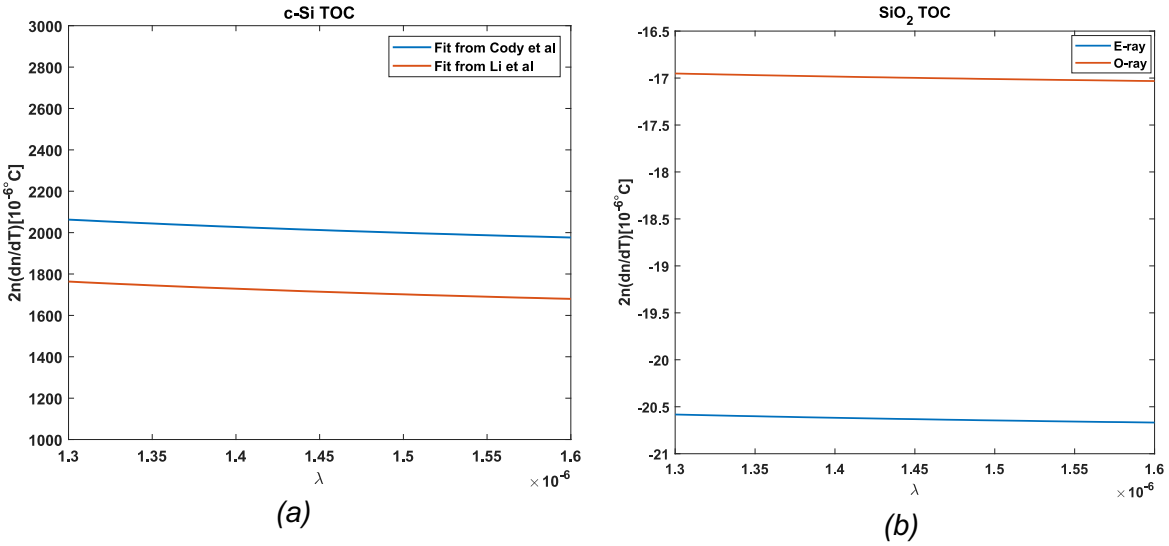

Figure 10. $2n(dn/dT)$ for (a) Si and (b) SiO_2

From these figures we can confirm the assumption of the low variability on the TOC over wavelength for Silica and Silicon [9]. The maximum difference for Silica was:

$$\max\left(2n\left(\frac{dn}{dt}\right)_{SiO_2}\right) - \min\left(2n\left(\frac{dn}{dt}\right)_{SiO_2}\right) = 0.080597$$

corresponding to a variation of 0.4% from the maximum value and for Silicon was:

$$\max\left(2n\left(\frac{dn}{dt}\right)_{c-Si}\right) - \min\left(2n\left(\frac{dn}{dt}\right)_{SiO_2}\right) = 86.3413$$

corresponding to a 4% variation from the maximum value.

Recent experimental data from [12] confirms those observations for Silicon and $\frac{dn}{dT}K^{-1}$ over the temperatures of 200 K, 250 K and 295 K, from $1.1\ \mu\mathrm{m}$ to $2\ \mu\mathrm{m}$, is shown in Figure 11.

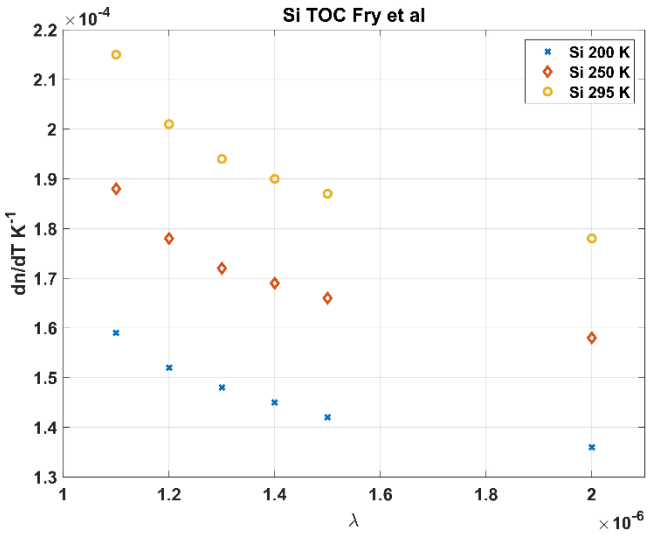

Figure 11. dn/dT^{-1} for Si. Values extracted from [12].

Optical switches based on single-stage *Mach-Zehnder interferometers* (MZIs), as shown in Figure 12, with two arms of equal length and a thermo optic phase shifter in one of the arms have shown good performance over a wide operating range [11][12].

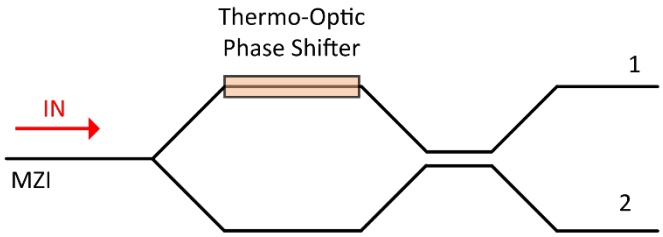

Figure 12. 1x2 Optical switch based on single-stage MZI and thermo-optic phase shifter.

Experimental validation conducted on these types of switches over the O, E, S, C and L-band [14] showed switching between output waveguides occurs with little variation on the applied electrical current, with the heating on the waveguides occurring due to the Joule Effect [15], further confirming the confirming the wideband nature of the thermo-optic effect. The experimental results on these switches are further highlighted for wavelengths from the O to the L band on Figures 13 to 15 and on Table 2 the contrast ratio, i.e the power ratio between two output states.

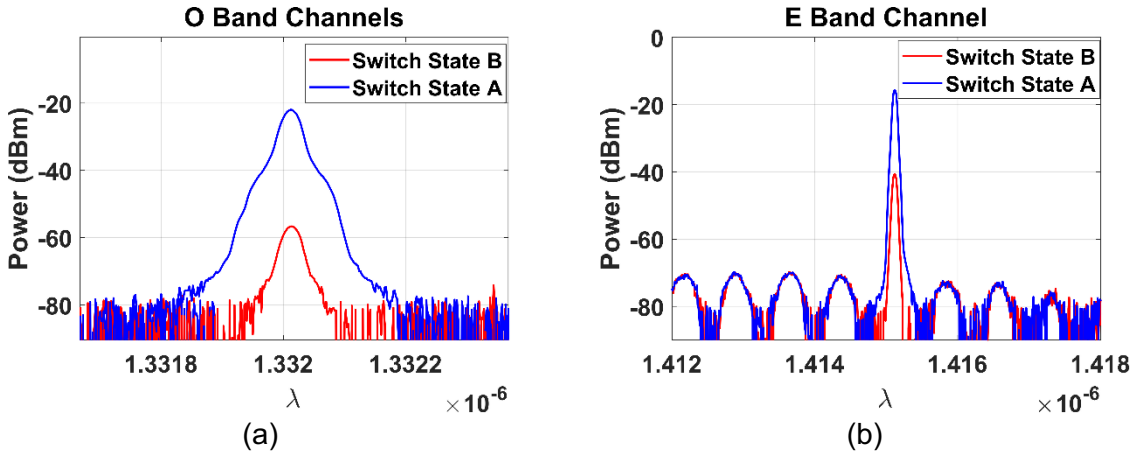

Figure 13. O (a) and E (b) bands contrast ratio.

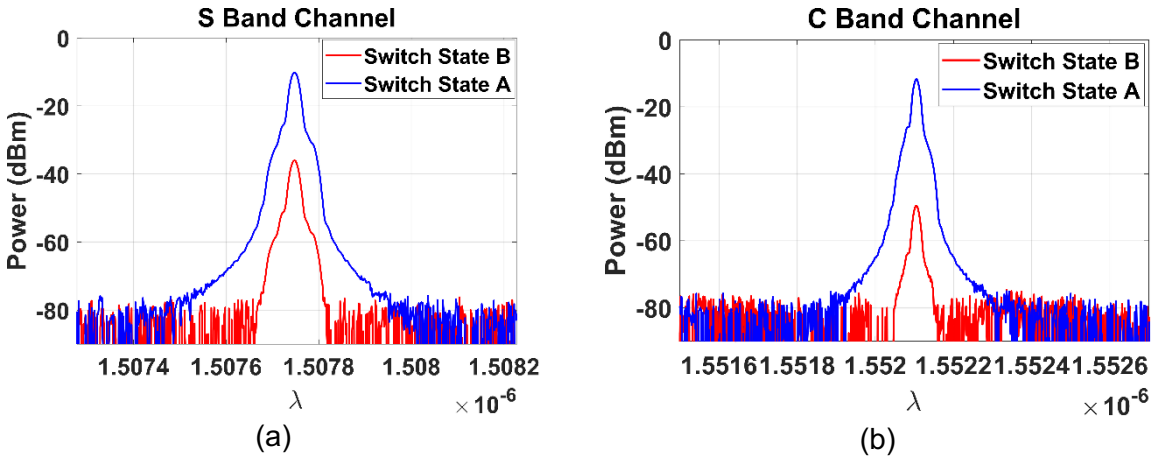

Figure 14. S (a) and C (b) bands contrast ratio.

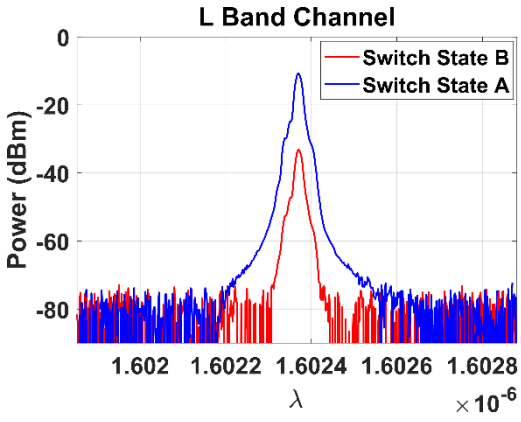

Figure 15. L-band contrast ratio

Band	Wavelength	Contrast Ratio
O	1332.02 nm	35.8 dB
E	1415.00 nm	24.9 dB
S	1507.70 nm	25.8 dB
C	1552.12nm	27.4 dB
L	1602.38 nm	26.2 dB

Table 2.Thermo-Optic switch Contrast Ratio

4. 1 x 2 photonic integrated wideband wavelength selective switch.

We have reported a photonic integrated WSS with wideband operation on [12] [13]. The WSS is a 1 x 2 device and designed with 40 channels with 100 GHz channel spacing with no wavelength crossings as seen from its layout on Figure 16. The WSS uses 1.5%Δ silica waveguides on a silicon substrate and it consists of a demultiplexer AWG, a switching section and a multiplexer AWG.

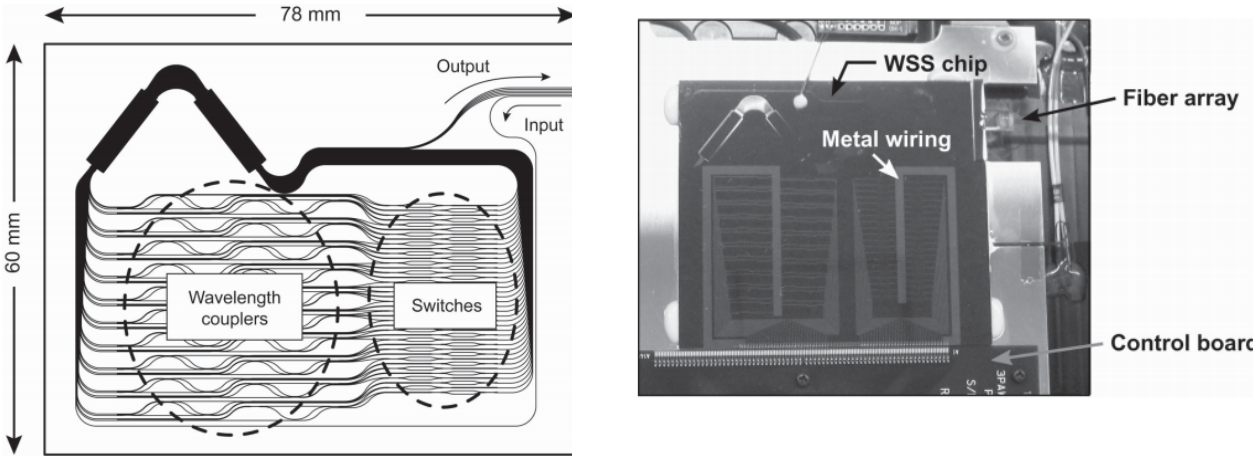

Figure 16. Layout and Photograph of the fabricated WSS

As described on section 3, the switching section consists of single-stage MZIs with two arms of equal length and thermo-optic phase shifters and MZIs with two arms of different lengths as wavelength couplers. The WSS is fully packaged and pigtailed with an embedded switch controller for selecting each of the multiband channels.

For assessing the *bit-error-rate* (BER) of the WSS the setup depicted on Figure 17 was used. On the C and L-bands a broadband *tunable laser source* (TLS) was used the generate a *continuous-wave* (CW) optical signal. After the CW source a *Mach-Zehnder modulator* (MZM) was used to externally modulate the laser light. The MZM was driven at 10 Gb/s or 35 Gb/s *non-return to zero on-off keying* (NRZ-OOK) data with a pattern length of $2^{31} - 1$. In Figures 17b and 17c we show the *optical signal-to-noise-ratio* (OSNR) at both outputs for the C and L-band. The measured OSNRs at both outputs were ≥ 47 dB.

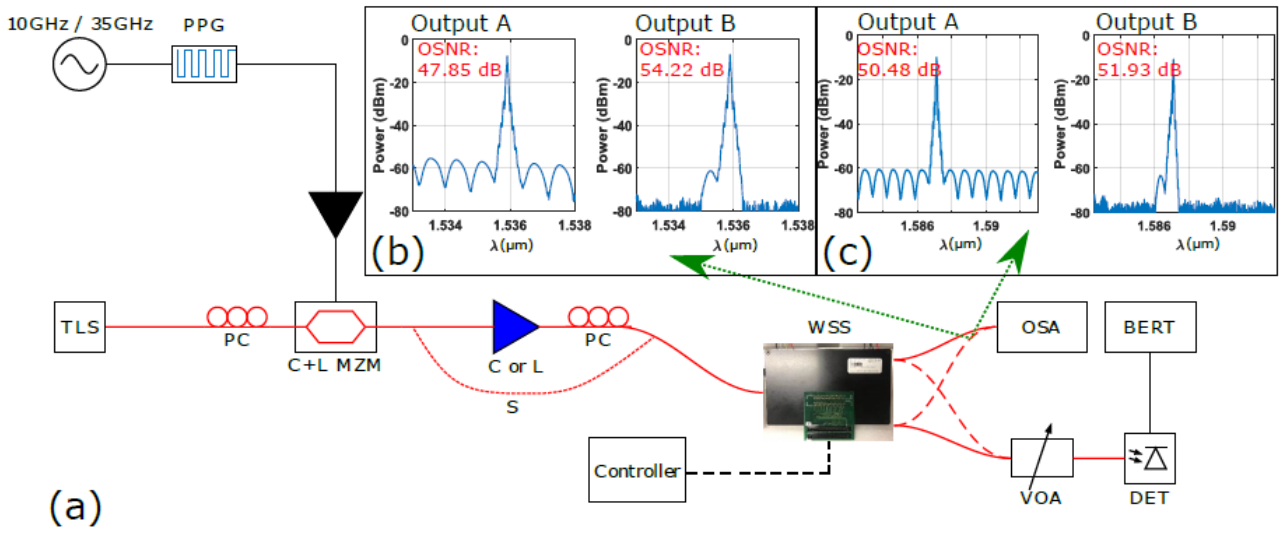

Figure 17. (a) BER assessment setup. (b) OSNR at the C-band. (c) OSNR at the L-band.

In Figures 18a, 18b, 18c, 18d and 18e the BER performance across the S, C and L-bands for 10 Gb/s and 35 Gb/s is presented. At 10 Gb/s in the C-band the power penalty at 10^{-9} is around 1 dB and negligible at the L-band. At 35 Gb/s we see a penalty of around 2 dB at the C-band and ranged from 0.5 dB to 3.5 dB at the L-band. In the S-band error free operation is also obtained with a penalty of around 0.5 dB at 10^{-9}.

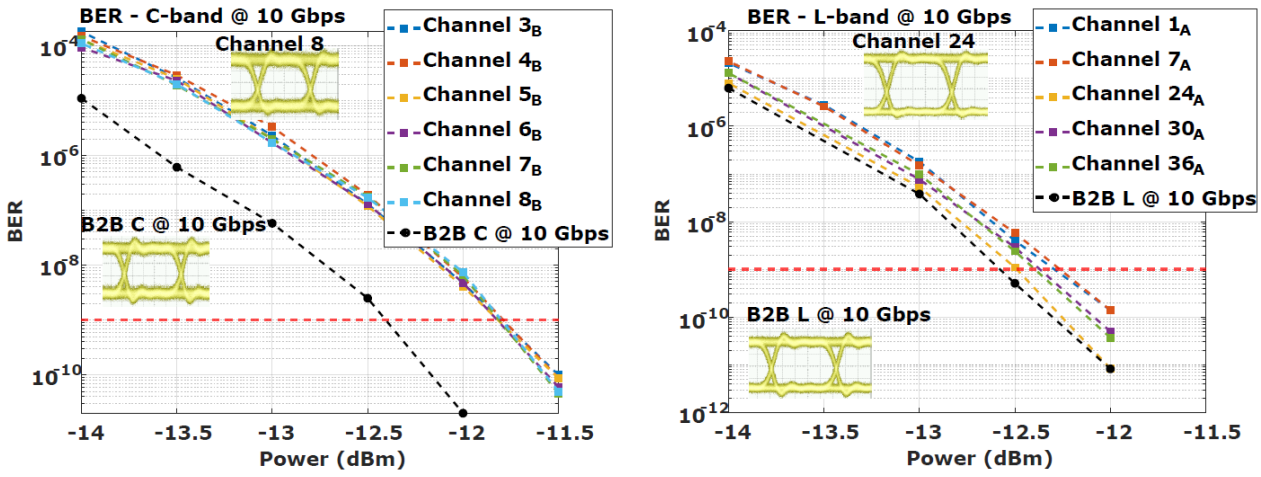

(a) (b)

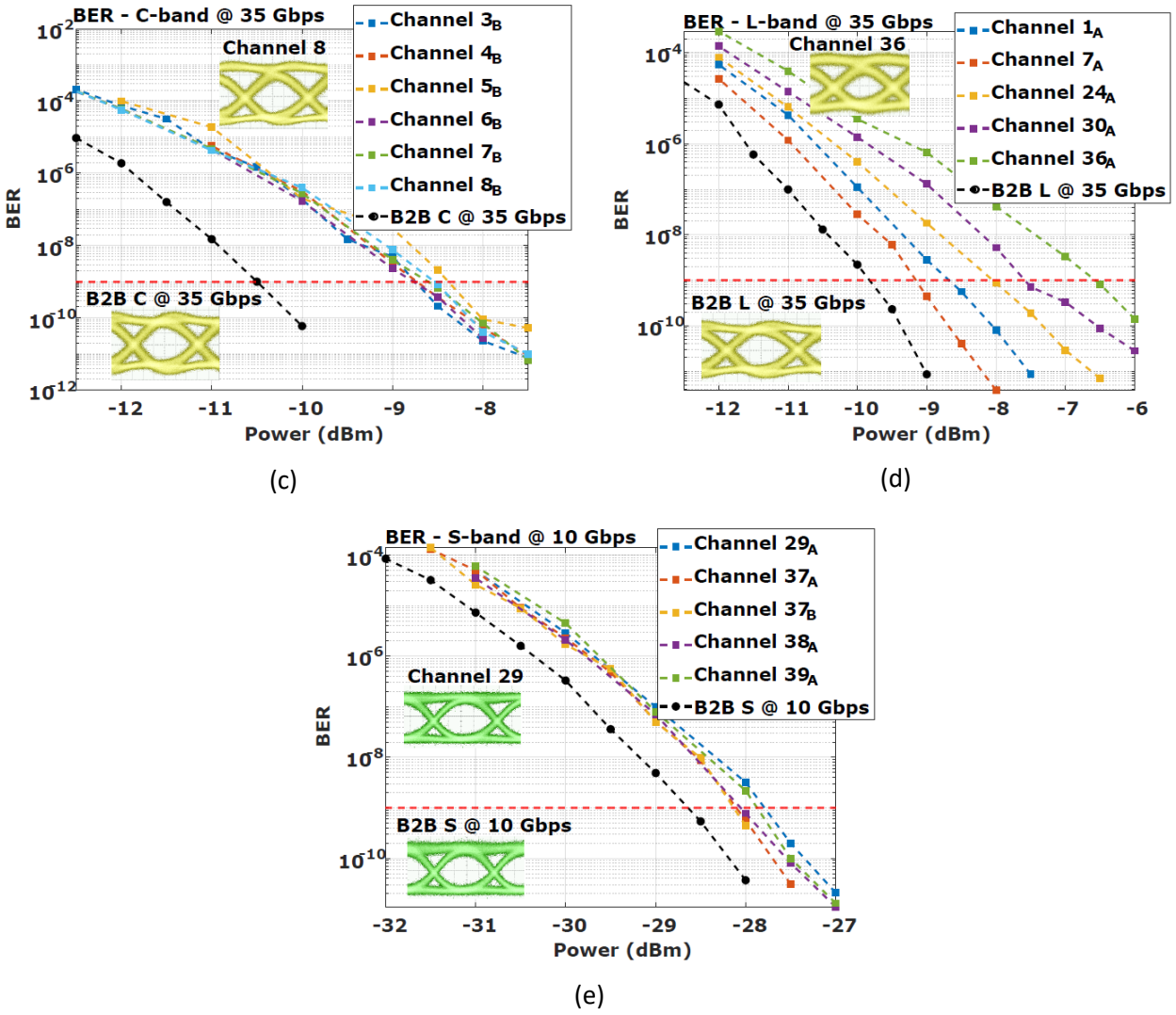

Figure 18. BER Results for the S-, C- and L-bands

This demonstrated device presents itself as viable alternative for future wideband networks, especially in networks and scenarios with less need for multidegree optical mesh connectivity.

5. Conclusion

In this document, a new architecture for add/drop switching nodes based on novel integrated photonic components were proposed with the items described in the previous sections being subject of the WON publications [2], [6], [13] and [14] listed on the references section.

In section 2 design methods and simulations for wideband demultiplexers and multiplexers were presented, and simulation results showed the feasibility of integrated echelle gratings for wideband operation. Furthermore, experimental results on AWGs on a 3-μm platform confirmed wideband operation with low insertion loss, low crosstalk and polarization independent operation across the S-, C- and L-bands.

In the following section, section 3, it was shown that switches making using of thermo-optic effect are a promising solution for wideband operation given the low variability of the thermo-optic coefficient

from the O- to the L-band on Silica and Silicon. Experimental results conducted on Silica waveguides on a silicon substrate further confirmed wideband operation for these types of switches.

Finally, on section 4, experimental results of a photonic integrated wavelength selective switch operating from S- to the L-Band showed a low BER penalty at 10 Gb/s and 35 Gb/s with NRZ OOK modulation and confirmed the potential for the deployment of this add/drop switching architecture in current and future wideband networks.

REFERENCES

[1] K. Prifti, X. Xue, N. Tessema, R. Stabile, and N. Calabretta, “Lossless Photonic Integrated Add-Drop Switch Node for Metro-Access Networks,” *IEEE Photon. Technol. Lett.*, vol. 32, no. 7, pp. 387–390, Apr. 2020, doi: 10.1109/LPT.2020.2975885.]

[2] N. Calabretta *et al.*, “Photonic Integrated WDM Cross-Connects for Telecom and Datacom Networks,” presented at the OECC, Taiwan, 2020.

[3] Y. Wang, J. Luo, K. Sun, B. Roth, and Z. Zhang, “Integrated Echelle Gratings as Compact Spectrometer for VIS and NIR Astronomy,” presented at the 2019 Conference on Lasers and Electro-Optics Europe & European Quantum Electronics Conference (CLEO/Europe-EQEC), Munich, Germany, 2019, doi: 10.1109/CLEOE-EQEC.2019.8871807.

[4] S. Janz *et al.*, “Planar Waveguide Echelle Gratings in Silica-On-Silicon,” *IEEE Photon. Technol. Lett.*, vol. 16, no. 2, pp. 503–505, Feb. 2004, doi: 10.1109/LPT.2003.823139.

[5] M. K. Smit and C. Van Dam, “PHASAR-based WDM-devices: Principles, design and applications,” *IEEE J. Select. Topics Quantum Electron.*, vol. 2, no. 2, pp. 236–250, Jun. 1996, doi: 10.1109/2944.577370.

[6] Y. Wang *et al.*, “Characterization of 1x12 AWG with 100 GHz channel spacing and low polarization sensitive based on 3-μm SOI platform,” p. 4.

[7] D. M. Marom *et al.*, “Wavelength-selective 1/spl times/K switches using free-space optics and MEMS micromirrors: theory, design, and implementation,” *J. Lightwave Technol.*, vol. 23, no. 4, pp. 1620–1630, Apr. 2005, doi: 10.1109/JLT.2005.844213.

[8] S. J. Chua and B. J. Li, “Introduction to optical switches,” in *Optical Switches*, Elsevier, 2010, pp. 1–4.

[9] L. Sirleto, G. Coppola, M. Iodice, M. Casalino, M. Gioffrè, and I. Rendina, “Thermo-optical switches,” in *Optical Switches*, Elsevier, 2010, pp. 61–96.

[10] Y. Ikuma, T. Mizuno, H. Takahashi, T. Ikeda, and H. Tsuda, “Low-loss Integrated 1×2 Gridless Wavelength Selective Switch With a Small Number of Waveguide Crossings,” in *European Conference and Exhibition on Optical Communication*, Amsterdam, 2012, p. Tu.3.E.5, doi: 10.1364/ECEOC.2012.Tu.3.E.5.

[11] E. Palik, *Handbook of Optical Constants of Solids*. Academic Press, 1997.

[12] B. J. Frey, D. B. Leviton, and T. J. Madison, “Temperature-dependent refractive index of silicon and germanium,” p. 10.

[13] R. M. G. Kraemer, F. Nakamura, Y. Wang, H. Tsuda, and N. Calabretta, “High Extinction Ratio and Low Crosstalk C and L-Band Photonic Integrated Wavelength Selective Switching,” in *2020 22nd International Conference on Transparent Optical Networks (ICTON)*, Bari, Italy, Jul. 2020, pp. 1–4, doi: 10.1109/ICTON51198.2020.9203210.

[14] R. Kraemer, F. Nakamura, H. Tsuda, and A. Napoli, “S-, C- and L-Band Photonic Integrated Wavelength Selective Switch,” p. 4.

[15] M. W. Pruessner, T. H. Stievater, M. S. Ferraro, and W. S. Rabinovich, “Thermo-optic tuning and switching in SOI waveguide Fabry-Perot microcavities,” *Opt. Express*, vol. 15, no. 12, p. 7557, Jun. 2007, doi: 10.1364/OE.15.007557.